Available online at www.sciencedirect.com

ScienceDirect

journal homepage: www.jfda-online.com

Original Article

Alleviating chronic kidney disease progression through modulating the critical genus of gut microbiota in a cisplatin-induced Lanyu pig model

Ya-Jane Lee [a,1], *Kuan-Yi Li* [b,1], *Pin-Jhu Wang* [b], *Hsiao-Wen Huang* [b], *Ming-Ju Chen* [b,c,*]

[a] *Institute of Veterinary Clinical Science, School of Veterinary Medicine, National Taiwan University, Taipei, Taiwan*
[b] *Department of Animal Science and Technology, National Taiwan University, Taipei, Taiwan*
[c] *Center for Biotechnology, National Taiwan University, Taipei, Taiwan*

ARTICLE INFO

Article history:
Received 2 July 2019
Received in revised form
22 September 2019
Accepted 1 October 2019
Available online 17 October 2019

Keywords:
Chronic kidney disease
Cisplatin
Gut microbiota
Lanyu pig
Probiotics

ABSTRACT

In the present study, we investigated the effects of Probiotic mix 1 (Pm1) with *Lactobacillus plantarum* subsp. *plantarum*, *Lactobacillus paracasei* subsp. *paracasei*, and *Streptococcus salivarius* subsp. *thermophilus* on preventing renal injury using a chronic kidney disease (CKD) minipig model previously developed in our lab using cisplatin-induced CKD in Lanyu pigs. The results indicated that the high dosage Pm1 (H.Pm1) group demonstrated lower incidence of lesions, including atrophy, mononuclear inflammation, cell infiltration, and interstitial fibrosis in renal tubules in hematoxylin and eosin (H&E) and Masson's trichrome stain. We further systematically investigated the preventing effect of Pm1. The H.Pm1 group decreased inflammatory cytokines production and increased the level of superoxide dismutase activity in plasma. The pigs fed with high dosage of Pm1 group also showed reduced both creatinine and blood urea nitrogen (BUN) when compared with the cisplatin group. Microbiota results indicated that Pm1-intervention not only reduced the abundance of Gram-negative bacteria but also affected the abundance of specific genera biomarkers, *Anaerovibrio*, *possible_genus*_SK018, *Holdemanella*, and *Lachnospiraceae*_UCG_010 in gut microbiota, leading to decreased inflammation and apoptosis in the kidney and further prevention/alleviation of the symptoms of CKD.

* *Corresponding author*. Department of Animal Science and Technology, National Taiwan University, No. 50 Lane 155 Sec. 3. Keelung Rd., Taipei, 106, Taiwan. Fax: +886 2 27324070.
E-mail address: cmj@ntu.edu.tw (M.-J. Chen).
[1] The authors contributed equally to this work.
https://doi.org/10.1016/j.jfda.2019.10.001

1. Introduction

The gut microbiota could help immunological tolerance to antigens from various nutrients or organisms, control nutrient uptake and metabolism, and prevent invasion of pathogenic organisms, which is important for regulating the normal function of the intestinal barrier [1–3]. Current findings suggest that the bacterial distribution and metabolites of the intestinal microbiota might positively affect disease pathogenesis [4], such as obesity [5], inflammatory digestive disease [6], and cancer [7]. The bacteria composition also plays an important role in the progression and complications of chronic kidney disease (CKD). CKD, characterized by a gradual loss of kidney function, is a global health issue that has a serious impact on affected individuals [8]. The intestinal microbiota may be the key factor that maintains the gastrointestinal tract in a chronic inflammatory state, as evidenced in patients with CKD, which contributes to the syndrome of uremia [9].

The modification of intestinal bacterial composition and metabolism might provide the solution for CKD deterioration [10]; thus, the interest in developing new research initiatives on probiotics in CKD have increased over the last decade, with the goal of fully exploring their therapeutic potentials [11,12]. The efficacy of probiotics to decrease uremic toxin production and to improve renal function has been investigated in both *in vitro* and *in vivo* models [13,14]. Most therapies targeting the colonic microenvironment in CKD aim to block lipopolysaccharide (LPS) or attenuate inflammation or target adsorption of uremic toxin end products of microbial fermentation [14,15].

The animal trial could assist to evaluate human diseases and to design adequate therapeutic interventions [16]. In CKD research, 5/6 nephrectomy in rodents has been a widely used model due to robust functional readouts and reliable induction. However, the surgery is complicated, time-consuming, and highly strain-specific in mice [17]. Although rodents are often used because of easy handling, there are numerous discrepancies between rodent and human models [18]. Minipigs are an appropriate biomedical model for humans due to many genetic and physiological similarities to humans, as well as the anatomical similarities in the kidneys and their microbiological characteristics, such as the composition of gut microbiota [19,20]. However, only a limited number of porcine CKD models have been developed [21,22].

Preselection of suitable probiotic strains based on their expression of functional biomarkers is crucial since the physiological functions of probiotics are highly strain specific [3]. In our previous study, three strains, *Lactobacillus plantarum* subsp. *plantarum* BCRC 12251, *Lactobacillus paracasei* subsp. *paracasei* BCRC 12188, and *Streptococcus salivarius* subsp. *thermophilus* BCRC 13869, were selected due to their abilities to reduce indoxyl sulfate (IS) *in vitro* [13]. IS, one of the gut-derived protein-bound uremic toxins, shows the positive correlation with the severity of renal dysfunction in CKD patients [23]. Combination of the strains (Pm1) demonstrated better IS removal than individual strains. *In vivo*, oral administration of Pm1 significantly suppressed the accumulation of IS in the serum, kidneys, and liver in a cisplatin-induced acute kidney injury model [13]. The Lanyu pig is an indigenous breed from Lanyu Islet, located southeast of Taiwan. The genotypic and phenotypic characteristics have been intensively studied and determined to be distinct from other pig breeds in Asia and Europe [24]. Taiwanese Lanyu pigs were found to be ideal for skin wound healing studies because of their small body size and stable wound healing features [25]. Since swine shares similar anatomic and physiologic characteristics with humans, in the present study, we investigated the effects of Pm1 on preventing CKD progression in the minipig using a cisplatin-induced CKD model previously developed in our lab [13]. The possible mechanisms related to anti-inflammation, anti-oxidation, and regulating gut microbiota were also investigated.

2. Methods

2.1. Bacterial strains

Pm1 consisted of *Lb. plantarum* subsp. *plantarum* BCRC 12251, *Lb. paracasei* subsp. *paracasei* BCRC 12188, and *S. salivarius* subsp. *thermophilus* BCRC 13869. The culture condition and preparation procedure of Pm1 followed the method as previously described [13]. Each strain was mass-produced using a 5-ton incubator and freeze-dried with skim milk powder as a cryoprotectant by Grape King Bio, Ltd. (Taoyuan, Taiwan) for the following animal study.

2.2. Cisplatin-induced CKD Lanyu pig model

Twelve 8-month-old Lanyu pigs from Taitung Animal Propagation Station (Taitung, Taiwan) were housed individually in pens under a natural light/dark cycle and environmental temperature, and with free access to food and water. Pigs with similar body weights were randomly divided into four groups of three animals each (control, CP, L.Pm1, and H.Pm1). Pigs in the L.Pm1 and H.Pm1 groups were administered Pm1 daily for 90 days before cisplatin injection and throughout the whole experiment period with 10^9 and 10^{10} CFU/kg feed, respectively; the other two groups were administered with skim milk powder instead. For induced CKD symptoms, cisplatin injection procedures were conducted following the methods as previously described with modifications [26]. Body surface area (BSA, m^2) of miniature pigs were calculated based on the body weight using the formula as previously described [27]. Pigs were injected intravenously via auricular vein with a low dosage of cisplatin (10 mg/m^2 BSA) seven consecutive times every two days beginning on the 91st day (day 0) and followed by a high dosage (30 mg/m^2 BSA) for two consecutive injections every two days. During this period, blood samples were collected at day 0, 4, 10, 14, and 16. After 9 cisplatin injections, blood samples were also collected at day 19, 25, 32, and 39. At the end of animal experiment, all pigs were sacrificed for collection of blood, feces, kidney, and cecum content samples. All animal experimental protocols were reviewed and approved by the Institutional Animal Care and Use Committee of National Taiwan University (Approval No: NTU-103-EL-32).

2.3. Analysis of blood urea nitrogen, creatinine, and IS in plasma

Blood urea nitrogen (BUN) and creatinine in plasma were assessed using a Vitros 350 analyzer (Ortho Clinical Diagnostics, Raritan, NJ, USA). The concentration of IS was measured by a high-performance liquid chromatography (HPLC) system (Jasco International Co. Ltd., Tokyo, Japan), equipped with quaternary gradient pump (PU-2089), coupled to a fluorescence detector (FP-2020) using Reprosil 100 C18 column (250 × 4.6 mm; 5 μm particle size; Dr. Maisch GmbH, Ammerbuch-Entringen, Germany). IS (Cayman Chemical Co., Ann Arbor, MI, USA) was dissolved in methanol as a standard solution. The mobile phase, which consistently mixed with sodium acetate buffer (pH 4.5) and acetonitrile (10:90, v/v), was delivered at flow rate of 1.3 mL/min. The excitation and emission wavelengths were set at 280 and 375 nm, respectively.

2.4. Evaluation of fecal bacterial flora

Fresh feces were collected on day 39, and the analysis was performed immediately after sampling. Fecal bacterial numbers of lactobacilli, bifidobacteria, *Escherichia coli*, and *Clostridium perfringens* were evaluated by Lactobacilli MRS agar (Neogen Corp., Lansing, MI, USA), *Bifidobacteria* iodoacetate medium-25 agar (Taiwan Prepared Media, Taipei, Taiwan), tryptose sulphite cycloserine agar (Neogen Corp.), and CHROMagar ECC (CHROMagar, Paris, France), respectively. The culture condition followed the method as previously described [28].

2.5. Histological examination

Kidney sections were stained with hematoxylin and eosin (H&E) and Masson's trichrome to evaluate kidney damage and fibrosis. Histopathological features were determined based on quantitatively different scores as follows: 0, absent; 1, mild (<10%); 2, mild to moderate (10–25%); 3, moderate (25–50%); 4, moderate to severe (50–75%); and 5, severe (>75%). The kidney lesions, including inflammation (grade 0–5) and fibrosis (grade 0–5) in the renal interstitium; atrophy (grade 0–5), degeneration (grade 0–5), necrosis (grade 0–5), regeneration (grade 0–5), and hyaline cast (grade 0–5) in the renal tubule; and dilation of Bowman's capsule (grade 0–5) in the renal corpuscle, were analyzed and scored by the pathologists. The kidney injury score of each individual was then calculated from the sum of each corresponding grade in the different parameters [29]. The full section of the kidneys at low power field to ensure the lesions which were consisted of the diffuse type. Subsequently, three randomly chosen, non-overlapping fields were then selected for evaluating the score of kidney lesions and summing up the score of each parameter as the kidney injury score. All morphological analyses were examined blindly by experienced pathologists. For Masson's trichrome staining, the area of the fibrotic lesion of the cortical interstitium was assessed using ImageJ v1.52a software (National Institutes of Health, Bethesda, MD, USA). Cellular apoptosis was evaluated by performing immunohistochemistry using the standard avidin-biotin immunoperoxidase method. The kidney sections were immunostained with cleaved caspase-3 antibodies. The immunohistochemistry staining was performed following the manufacturer's protocol (Ultravision Detection System, Thermo Fisher Scientific, Waltham, MA, USA). The cleaved caspase-3 positive area (%) was quantified by ImageJ v1.52a software.

2.6. Analyses of plasma cytokines

Tumor necrosis factor (TNF)-α and interleukin (IL)-6 levels in plasma were measured using commercial enzyme-linked immunosorbent assay (ELISA) kits (porcine cytokine kit, R&D system, Minneapolis, MN, USA) according to the manufacturer's instructions.

2.7. Analyses of antioxidative-related enzyme activity in plasma and kidney tissues

The levels of catalase (CAT), superoxide dismutase (SOD), and glutathione peroxidase (GPx) in plasma and kidneys were determined using a commercial kit (Cayman Chemical Co., Ann Arbor, MI, USA) according to the manufacturer's instructions.

2.8. Microbiota analysis

Total genomic DNA was extracted from approximately 200 mg of cecum content samples with the QIAamp DNA Stool Mini Kit (Qiagen, Hilden, Germany) according to the manufacturer's instructions. The V3–V4 regions of 16S rRNA genes were amplified by universe primers 341F (5′-CCTACGGGNGGCWGCAG-3′) and 805R (5′-GACTACHVGGGTATCTAATCC-3′) with the barcodes. Barcoded amplicons were analyzed and sequenced using the Illumina MiSeq paired-end sequencing platform. Effective tags were obtained followed the procedures as previously described [5]. Sequences with ≥97% similarity were assigned to the same operational taxonomic units (OTUs) by Uparse v7.0.1001 software [30]. Taxonomic annotation of the representative sequence for each OTU was performed using the Ribosomal Database Project (RDP) classifier v2.2 against the Silva v128 database [31,32]. OTU abundance information was normalized using a standard sequence number corresponding to the sample with the least sequences. Subsequent analyses were performed by this normalized data. The alpha diversity (chao 1 richness estimator and Shannon's diversity index) and partial least squares discriminant analysis (PLS-DA) were analyzed with QIIME v1.7.0 and R v2.15.3 software. The linear discriminant analysis (LDA) effect size (LEfSe) algorithm was executed for biomarker discovery to identify differential enrichment of abundant taxa between groups [33]. Microbial biomarkers with log-transformed LDA scores greater than 2 were retained for subsequent plotting.

2.9. Statistical analysis

All values are given as mean ± standard error of the mean (SEM). Nonparametric Mann-Whitney U test was executed for all the phenotypic and next generation sequencing (NGS) data to identify significant difference compared with control and

CP group, respectively. Bacterial networks were constructed by Spearman's correlation analysis to clarify the correlation between biomarkers at the genus level, as well as between biomarkers and blood biochemical values. All statistical analyses were performed by Statistical Analysis System v9.4 (SAS Institute Inc., Cary, NC, USA) and R software.

3. Results

3.1. *Pretreatment of Pm1 prevents the symptom of the cisplatin-induced renal injury in minipig models*

First, we investigated the effects of Pm1 on food intake and kidney/body weight ratio of the cisplatin-induced renal injury minipigs. Results indicated that the cisplatin treatment (CP group) could significantly reduce kidney/body weight ratio in the minipigs (Fig. 1A). The pretreatment of 10^{10} CFU/kg feed Pm1 (H.Pm1 group) could prevent the decrease in the daily food intake and kidney/body weight ratio of the minipigs significantly after the cisplatin treatment (Fig. 1A).

We then determined the BUN, creatinine, and IS levels in plasma. The cisplatin treatment (CP group) significantly increased both plasma BUN and creatinine and reached 27.0 mg/dL (8.0 mg/dL for the normal control) and 4.4 mg/dL (1.3 mg/dL for the normal control) at day 19, respectively. Pretreatment of high-dose Pm1 could decrease levels of the plasma BUN and creatinine through all the experimental period as compared with the CP group (Fig. 1B). IS levels in plasma were elevated in the CP group as compared to the control counterparts. This increase in plasma IS level showed the trend to be suppressed when the minipigs had received Pm1 (Fig. 1C).

Consequently, we observed H&E stained kidney sections of the minipigs (Fig. 2A). Since no obvious gross lesion was observed in each pig, both kidneys were trimmed at the central part for the histopathologic evaluation with the sections of capsule, cortex, medulla, and papilla. The renal sections of

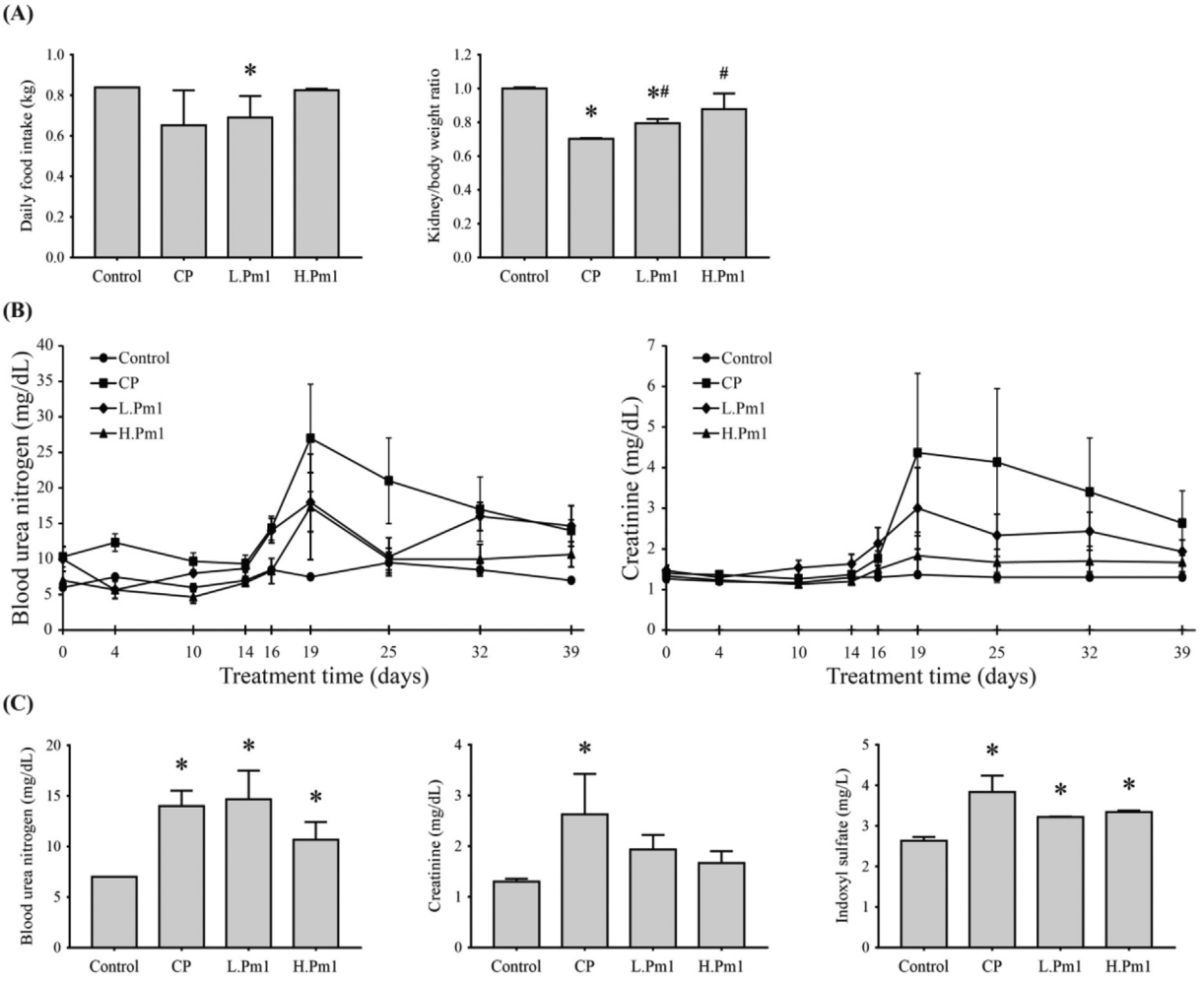

Fig. 1 – Administration of Pm1 effect on daily food intake, uremic toxins, and kidney in a cisplatin-induced renal injury Lanyu pig model. The effect of Pm1 on the (A) daily food intake and kidney/body weight ratio and; (B) plasma blood urea nitrogen (BUN) and creatinine in minipigs are revealed. (C) The plasma BUN, creatinine, and indoxyl sulfate on the 39th treatment day are shown. The data are presented as mean ± SEM. Symbols indicate significant difference compared with the control ($^{*}P < 0.1$) and CP groups ($^{\#}P < 0.1$), respectively.

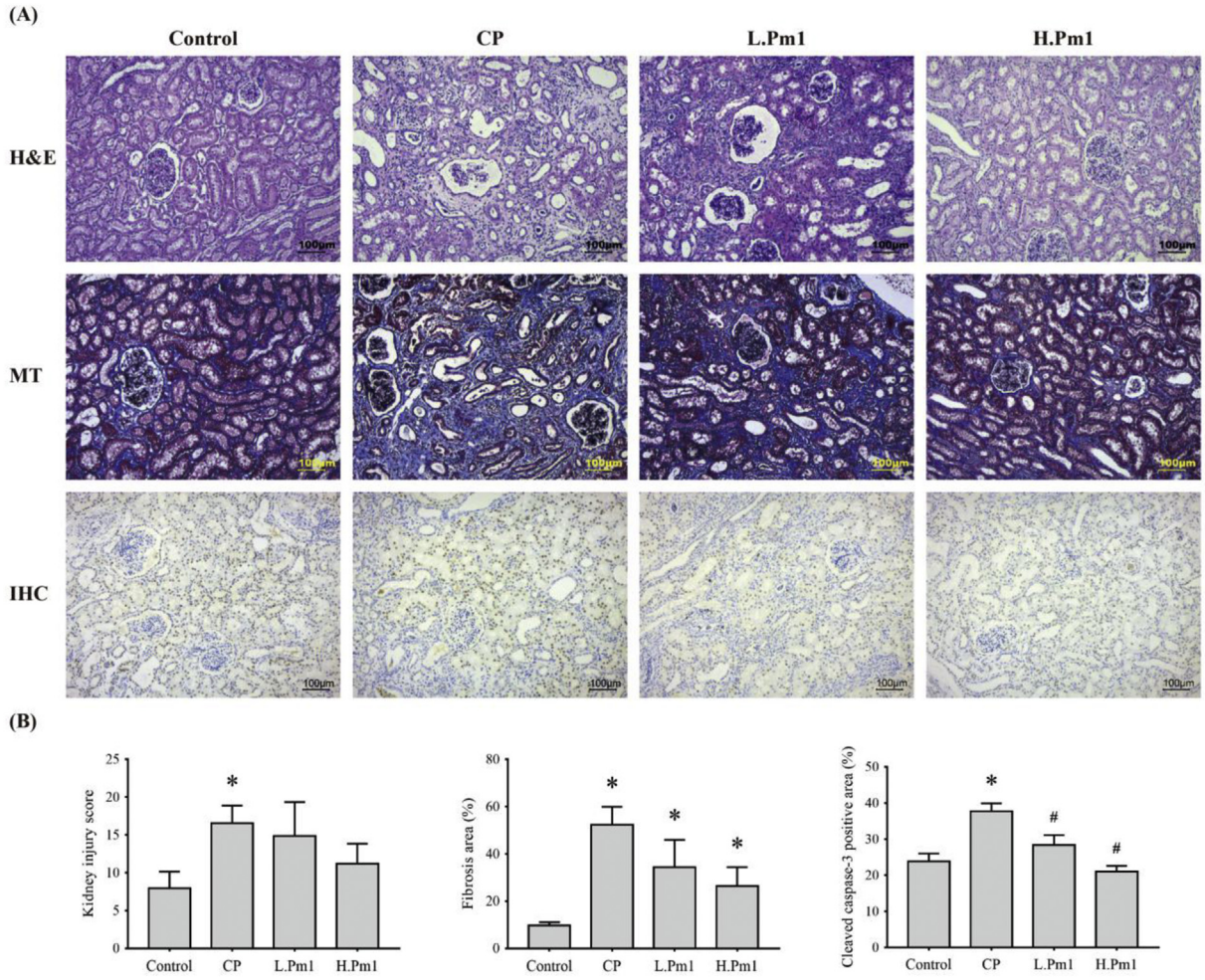

Fig. 2 – Pretreatment of Pm1 prevents the symptom of the cisplatin-induced renal injury and cell apoptosis in the chronic kidney disease minipigs. (A) The result of histopathology of kidney sections with hematoxylin and eosin (H&E) staining, and Masson's trichrome (MT) stain, and immunohistochemistry (IHC) staining for cleaved caspase-3 are shown. Scale bar = 100 μm. (B) Bars represent quantitative analysis of kidney injury score and interstitial fibrosis area. The data are presented as mean ± SEM. Symbol indicates significant difference compared with control (*P < 0.1) and CP groups (#P < 0.1), respectively.

the control minipigs showed normal parenchyma. The renal corpuscles appear to be morphologically normal with a double walled Bowman's capsule surrounding the glomerulus. Proximal and distal convoluted tubules can also be seen (Fig. 2A). After cisplatin treatment, the kidneys reveal degenerative changes, including tubular cell atrophy and cystic dilatation. Interstitial expansion of kidneys was also prominent in the cisplatin-treated minipigs (Fig. 2A). In Pm1-treated animals, interstitial expansion was less than that in the CP group and the tubular back-to-back structure was relatively well preserved (Fig. 2A). The tubular injuries evoked by cisplatin were reduced by pretreatment of Pm1. The kidney injury score indicated that administration of 10^9 and 10^{10} CFU Pm1 prevented the cisplatin-induced kidney injury (Fig. 2B).

The fibrosis area of kidney tissue was also evaluated using Masson's trichrome staining on the 23rd day after cisplatin induction. The connective tissues with blue staining were deposited significantly on renal tubulointerstitium in the CP group indicating severe tubulointerstitial fibrosis (Fig. 2A). Pretreated Pm1 reduced the tubulointerstitial fibrosis in the kidneys on the 23rd day after cisplatin induction. The average reduced area of kidney tubulointerstitial fibrosis for the high-dose groups was 26% of that in the CP counterparts (Fig. 2B).

3.2. *Pm1 prevents the symptom of cisplatin-induced renal injury through modulating caspase-3, inflammatory cytokines, and anti-oxidative enzymes*

Additionally, caspase activation, a key step in the genesis of renal cell apoptosis, was also determined [34]. Results of localized caspase-3 immunohistochemistry indicated that the CP group exhibited significant accumulation of caspase-3 in the glomeruli, tubules, and interstitium in the kidney of renal injury Lanyu pigs. The caspase-3 level in renal cells evoked by cisplatin was reduced by pretreatment of Pm1 (Fig. 2A). Additional quantification of the cleaved caspase-3 positive

area by ImageJ software, the Pm1 groups also demonstrated significantly smaller positive areas than the cisplatin counterpart (Fig. 2B), indicating the preventing capability of Pm1 for the apoptosis of renal cells induced by cisplatin.

We next investigated the possible mechanisms by which Pm1 prevented the symptom of cisplatin-induced renal injury. First, we studied the levels of proinflammatory cytokines, TNF-α and IL-6, in plasma. Results indicated that the CP group had higher TNF-α and IL-6 than the control counterpart. Pretreatment with Pm1 demonstrated a tendency to reduce these two proinflammatory cytokines without statistical significance as compared with the CP group (Fig. 3A).

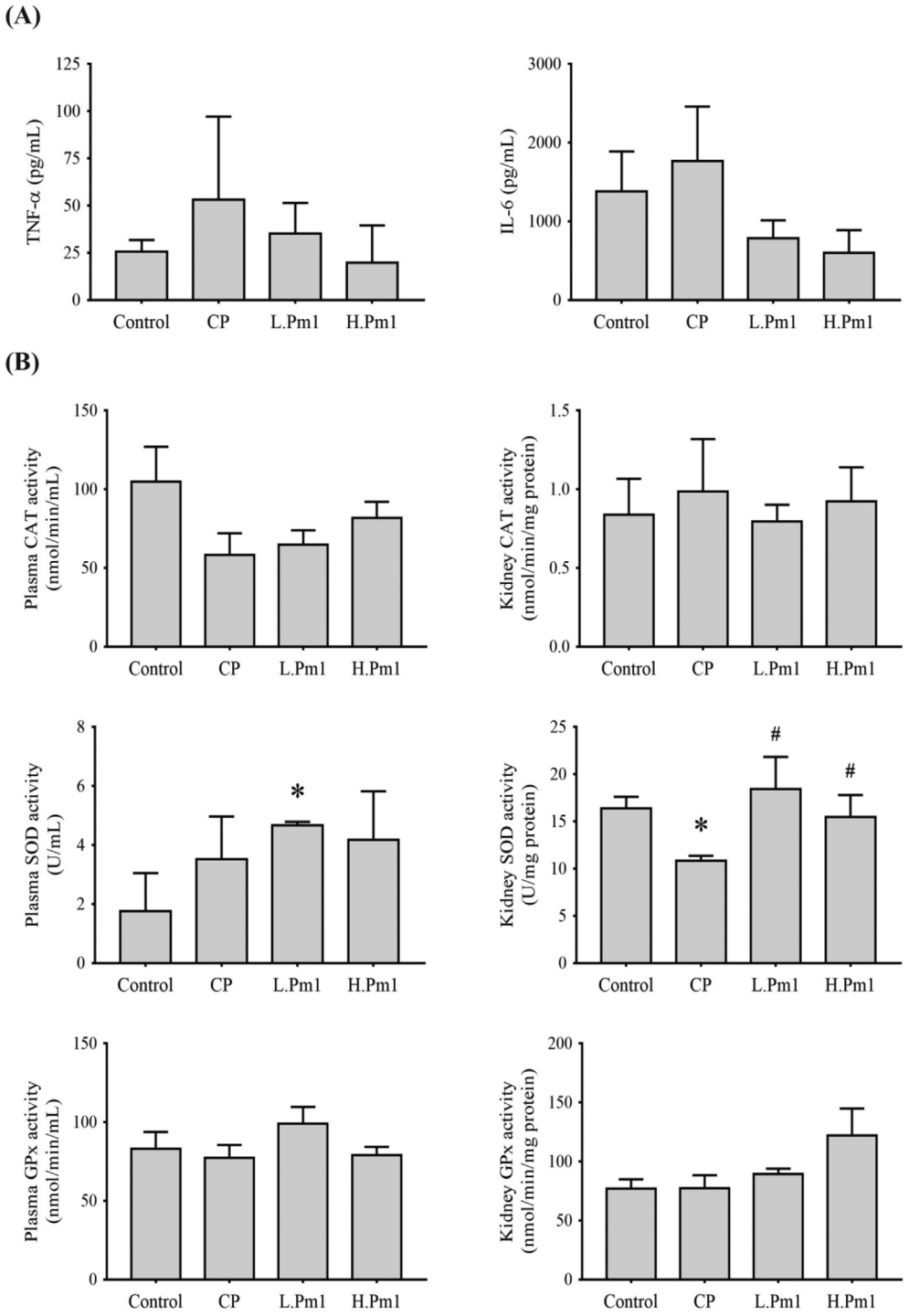

Fig. 3 – The effect of Pm1 intervention on inflammatory cytokines and anti-oxidative enzymes in the renal injury minipigs. Bars represent the effect of administration of Pm1 on (A) plasma inflammatory cytokines, TNF-α and IL-6, and (B) anti-oxidative enzyme activities, catalase (CAT), superoxide dismutase (SOD), and glutathione peroxidase (GPx) of plasma and kidney in a cisplatin-induced renal injury Lanyu pig model. The data are presented as mean ± SEM. Symbols indicate significant difference compared with control group ($^{*}P < 0.1$) and CP group ($^{\#}P < 0.1$), respectively.

We also measured the activities of major enzymes participating in free radical metabolism (CAT, SOD, and GPx) in plasma and kidney tissues. Results indicated that the CP group has a significantly lower SOD in the kidney as compared to other groups. Pretreatment with Pm1 increased the levels of SOD in the kidney and plasma when compared to CP group, while no difference was observed in CAT and GPx activity among the experimental groups (Fig. 3B).

3.3. *Pm1 intervention changed significantly enriched taxa in the cecum of the cisplatin-induced renal injury in a minipig model*

We then studied whether modulating effects of Pm1 on renal cell apoptosis, anti-oxidation, and inflammation were associated with changes in the gut microbiota. In fecal microbiota, the Pm1 administration group had a greater proportion of *Lactobacterium* and *Bifidobacterium* while significantly less *Clostridium* when compared with the cisplatin group (Table 1). In total, NGS results showed that a total of 1,956,259 effective tags were obtained from 3,458,032 raw paired-end reads. First, Pm1 administration showed a significant increase in Chao 1 richness estimator and the trend to increase Shannon's diversity index than other tested groups (Fig. 4A). A Venn diagram, reflecting the distribution of OTUs of gut microbiota in all tested groups, indicated that 975 (72.5%) of total 1344 OTUs were overlapped among four tested groups. Up to 12, 40, 8, and 9 OTUs only existed in the gut of the control, CP, L.Pm1, and H.Pm1 groups, respectively (Fig. 4B).

To clarify the role of Pm1 in alteration of intestinal microbiota, we also analyzed the abundance of specific bacterial taxa in the cecum. The abundance of Gram-negative bacteria (except *Ruminococcaceae*_UCG_005) was highest in the CP group (40.27%) than in the control group (32.44%), L.Pm1 group (24.43%), and H.Pm1 group (25.95%) in the top 10 predominant genera (Fig. 4C). The top 10 of specific genera showed that CP intervention could significantly reduce the abundance of *Prevotella*_9 and *Prevotellaceae*_NK3831_group and increase *Bacteroides* and *Fusobacterium* as compared with the control group, whereas Pm1 treatment could restore the microbiota toward the control group (Fig. 4C). Although heatmap results also showed a similar trend that Pm1 intervention could skew the microbiota toward the normal control, a diverse genera abundance was observed among the tested groups (Fig. 4D). Thus, we further evaluated the gut microbiota composition among all groups using the PLS-DA method. PLS-DA plot showed that PLS1 and PLS2 explained 15.00% and 9.25% of variation of gut microbiota composition, respectively. A significant separation in PLS1 and PLS2 among each group was observed (Fig. 4E). These findings indicated that the composition of gut microbiota, which has been assumed to be in a dysbiotic state due to cisplatin treatment, could be modulated through Pm1 administration to an intermediate configuration.

3.4. *Pm1 affected BUN and creatinine through manipulating the network of co-occurring genus biomarkers*

To further identify the specific bacterial taxa that were statistically differential as the biomarker between the H.Pm1 and CP groups, the LEfSe algorithm was used for biomarker discovery. A total of 35 influential taxonomic clades were recognized, and 18 genus biomarkers were obtained (Fig. 5A and B). With cisplatin treatment, the most impacted taxa in the CP group were the genera *Bacteroides*, *Lachnospiraceae*_UCG_010, *Alistipes*, and *Ruminococcaceae*_UCG004. Administrating Pm1 specifically influenced 22 taxonomic clades including the genera *Prevotella*_9, *Anaerovibrio*, *possible_genus*_Sk018, *Lachnospiraceae*_UCG_003, [*Eubacterium*]_*ruminantium*_group, *Oscillospira*, [*Eubacterium*]_*fissicatena*_group, *Ruminococcaceae*_UCG_009, *Coprococcus*_2, *Lachnospiraceae*_NK4A136_group, *Anaeroplasma*, *Lachnospira*, *Holdemanella*, and *Cuneatibacter* in the pigs.

After identifying the specific bacterial taxa as the biomarker between the H.Pm1 and CP groups, we aimed to determine whether there were any specific bacterial interactions among these biomarkers. Thus, we constructed a module of the microbiome network among 18 genera correlated with levels of BUN and creatinine. The BUN level was positively correlated with the biomarker *Lachnospiraceae*_UCG_010 and negatively correlated with *Anaerovibrio*, *possible_genus*_Sk018, and *Holdemanella* ($P < 0.05$) (Fig. 6A). Among the bacterial network, *Lachnospiraceae*_UCG_010 was also negatively correlated with *Anaerovibrio*, *possible_genus*_Sk018, and *Holdemanella* ($P < 0.05$) (Fig. 6A). Similar results were found in the creatinine. Creatinine levels were negatively correlated with *Holdemanella* ($P < 0.05$), indicating that physiologically important microbes may be influential at narrower taxonomic levels. The relative abundances of these four genera were consistent with the above findings (Fig. 6B). The H.Pm1 group showed significantly higher relative abundances of *Anaerovibrio* and *possible_genus*_Sk018, and significantly lower relative abundances of *Lachnospiraceae*_UCG_010 than the CP group. Administration of Pm1 also showed the tendency to increase the relative abundances of genus *Holdemanella*.

Table 1 – Effect of Pm1 treatment on fecal microbiota in a cisplatin-induced renal injury minipig model.

	Lactobacilli	Bifidobacteria	*Escherichia coli*	*Clostridium perfringens*
Control	$9.95 \pm 4.38 \times 10^8$	$2.33 \pm 2.06 \times 10^8$	$1.25 \pm 0.24 \times 10^8$	$4.30 \pm 0.60 \times 10^6$
CP	$4.79 \pm 2.94 \times 10^8$	$5.40 \pm 1.63 \times 10^7$	$4.65 \pm 3.30 \times 10^7$	$5.08 \pm 1.12 \times 10^6$
L.Pm1	$7.79 \pm 5.33 \times 10^8$	$3.15 \pm 1.40 \times 10^8$	$2.50 \pm 1.00 \times 10^{7*}$	$8.47 \pm 1.70 \times 10^{5*\#}$
H.Pm1	$7.92 \pm 3.26 \times 10^8$	$1.86 \pm 1.40 \times 10^8$	$7.40 \pm 3.80 \times 10^7$	$9.70 \pm 1.21 \times 10^{5*\#}$

Control: pigs fed with normal diet; CP: cisplatin-induced pigs fed with normal diet; L.Pm1: cisplatin-induced pigs fed with 10^9 CFU/kg feed Pm1; H.Pm1: cisplatin-induced pigs fed with 10^{10} CFU/kg feed Pm1. The data are presented as mean ± SEM (CFU/g). Symbols indicate significant difference compared with the control group ($^*P < 0.1$) and CP group ($^\#P < 0.1$), respectively.

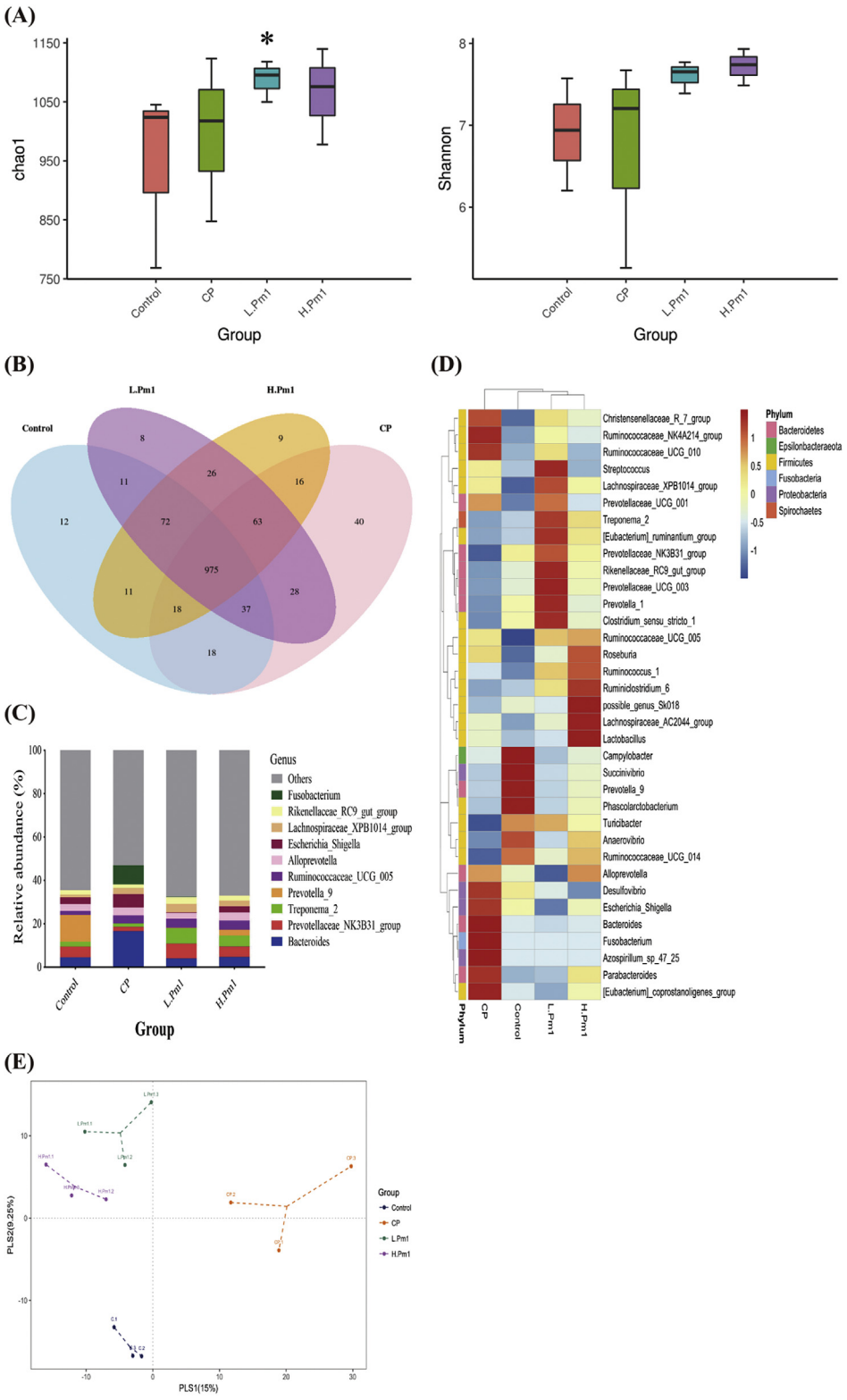

Fig. 4 – Gut microbiota dysbiosis in the renal injury minipigs is restored by Pm1 intervention. (A) The chao 1 richness estimator and Shannon's diversity index are shown with symbols indicating significant difference compared with the control group (*P < 0.1). (B) Venn diagram shows the distribution of OTUs of gut microbiota in four groups. Gut microbiota composition are presented as (C) bar chart and (D) heatmap based on the relative abundance at genus level. (E) Partial least squares discriminant analysis (PLS-DA) plot based on the relative abundance of bacterial taxa indicates administration of Pm1 manipulates microbiota composition among groups.

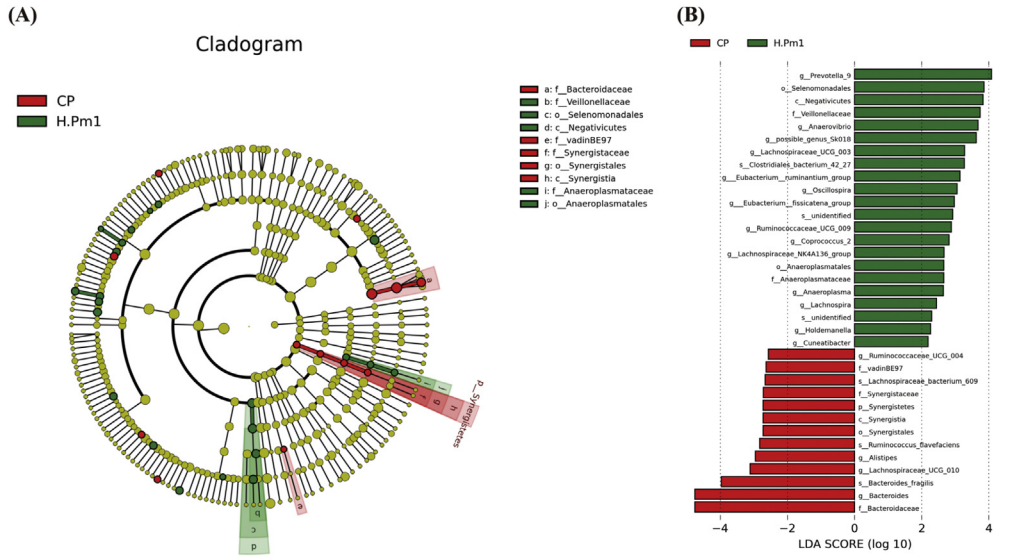

Fig. 5 – Significant differential biomarkers are identified using linear discriminant analysis (LDA) effect size (LEfSe) algorithm. (A) LEfSe cladogram and (B) log-transformed LDA score illustrate differential enrichment of biomarkers between CP and H.Pm1 groups.

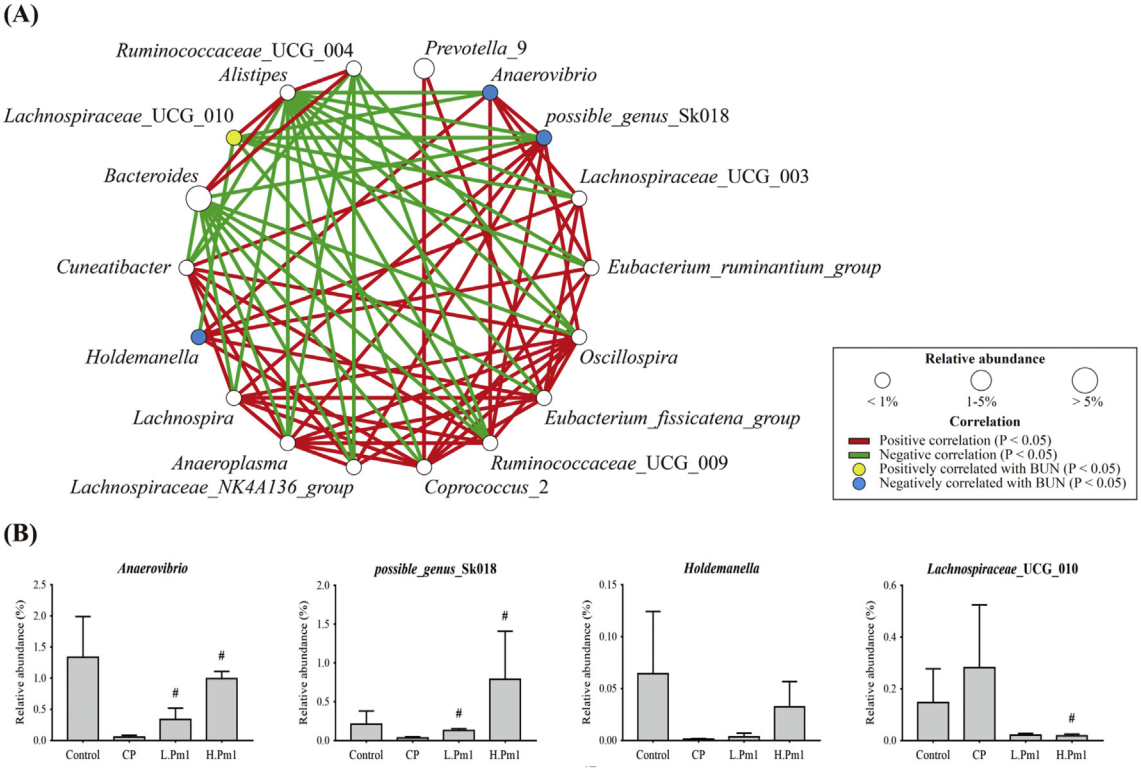

Fig. 6 – Alleviating chronic kidney disease progression through modulating the critical biomarkers of gut microbiota in the renal injury minipigs. (A) Bacterial networks of pig gut microbiota show the correlation relationships among 18 genus biomarkers in CP and H.Pm1 groups. Each node represents a genus biomarker, and the size of it corresponds to relative abundance. Yellow and blue nodes show significantly positive and negative correlations with blood urea nitrogen (BUN) ($P < 0.05$), respectively. Red and green edges indicated the significantly positive and negative correlation between biomarkers ($P < 0.05$), respectively. (B) Bar charts of four biomarkers significantly correlated with BUN in CP and H.Pm1 groups are shown. The data are presented as mean ± SEM. Symbol indicates significant difference compared with CP group ($^{\#}P < 0.1$).

4. Discussion

In the present study, we evaluated the effect of Pm1 on preventing renal dysfunction and renal proximal tubular cell (RPTC) apoptosis using a cisplatin-inducing renal injury pig model. We then systematically verified the possible mechanism contributing to the preventing effects in CKD, further underscoring the importance of the tripartite relationship among the host, microbiota, and metabolites.

First, we observed that the Lanyu pigs treated with cisplatin showed a decrease in daily food intake and kidney/body weight ratio. Both features were attenuated but not completely prevented by pretreatment with 10^{10} CFU/kg feed Pm1. Cisplatin, a platinum compound, has been widely used as an effective chemotherapeutic agent for many carcinomas, sarcomas, and lymphomas due to its high activity to bind with DNA and form cross-linking contributing to inhibit DNA synthesis and replication [35]. However, the major limitation and concerns in the use of cisplatin are the side effects including nausea, vomiting, and nephrotoxicity, which could also lose appetite and reduce the food intake. The side effects evolve slowly and predictably after initial and repeated exposure of cisplatin [36]. The renal dysfunction features, including high levels of BUN and creatinine in plasma, interstitial fibrosis and tubular injuries in cisplatin-induced renal injury was reduced by Pm1 pretreatment, which was accompanied by suppression of caspase-3 and proinflammatory cytokines production. Caspase-3 is one of the most important members of the caspase enzyme family, having a crucial role in both intrinsic and extrinsic apoptosis pathways [37,38]. Several studies demonstrated that caspase-3 was activated in renal cell lines with cisplatin. Upregulated apoptosis in kidneys is likely to be caspase-3-dependent. Caspase-3 also correlated with inflammation and fibrosis in kidneys [37].

Consistent with suppression of caspase-3, the production of proinflammatory cytokines (TNF-α, IL-6) also decreased in the cisplatin-treated pigs given Pm1. Earlier reports have shown that critical proinflammatory mediators, such as TNF-α contribute to tissue damage [39]. This evidence suggests that Pm-1 has a potent reduction of caspase-3 and proinflammatory cytokines, which may lead to inhibition of inflammation and apoptosis in the cisplatin-treated pigs. Several studies suggested that the presence of specific probiotic strains could move cytokine production from a proinflammatory to an anti-inflammatory profile [39]. Blockade/inhibition of caspase-3 in progress of renal injury by Pm1 pretreatment might provide a novel approach to the prevention/alleviation of renal injury by controlling in appropriate apoptosis of renal cells.

In accordance with the anti-inflammatory and antioxidative effects of Pm1, we observed that the abundance of renal toxin and inflammation-associated bacteria in intestinal microbiota were regulated by the Pm1 intervention. The study revealed higher microbiota richness and diversity as presented by alpha diversity indexes in the Pm1 groups compared with the CP group. The result was parallel with the previous study, which indicated that CKD rats had lower genus richness and relative abundance using a 5/6 nephrectomy CKD rat model [40].

Additionally, shifts in the microbial community structure may also play a crucial role by Pm1 in CKD prevention. We noticed that the top 10 predominant genera, occupying 40.27% relative abundance in the CP group, were almost all Gram-negative bacteria. Changes in the composition of the intestinal microbiota toward Gram-negative, pathogenic bacteria could generate the intestinal immune system in the direction of a proinflammatory response and increase the production of LPS, a major component of the Gram-negative bacterial outer membrane [41]. Dysbiosis of microbiota also led to an increase in intestinal permeability and disruption of its barrier function which may subsequently result in translocation of LPS and bacteria into the internal environment and the alteration of toxic metabolites that contribute to loss of kidney function due to uremic toxicity and inflammation [40,41]. Loss of kidney function could inversely cause the production of urea in the gastrointestinal tract. Urea could be hydrolyzed by certain microorganisms into ammonia and influence the growth of commensal microorganisms [42].

Some Gram-negative bacteria have been found to be associated with human diseases, such as *Fusobacterium*, which was higher in the CP group than other tested groups. *Fusobacterium* within the family Bacteroidaceae, found mainly in the mouth, upper respiratory tract, gastrointestinal tract, and female genital tract, cause several human diseases, including periodontal diseases, Lemierre's syndrome, and topical skin ulcers [43]. Recent studies have indicated that *Fusobacterium* may be correlated to colon cancer and ulcerative colitis [44]. *Fusobacterium* was also reported in hemodialysis patient [45]. The Pm1 groups in our study harbored more diverse and shared more similar microbial communities to the normal control group than did the CP group. Many commensal or beneficial microbes, such as *Prevotella* and *Ruminococcaceae*, depleted in the CP group, were restored in the Pm1 group. The *Prevotellaceae* family was found to have a decreased abundance in uremic animals and the CKD patients [40,46]. Firmicutes genus *Ruminococcus* was associated with improved kidney function as measured by creatinine clearance [47]. These beneficial bacteria also produce short-chain fatty acids (SCFAs), especially butyrate acid, which has multiple critical roles in the maintenance of human health, including producing intestinal epithelial nutrition and energy components, reducing the severity level of inflammation, and enhancing intestinal barrier functions [48,49]. The findings showed that pretreatment with Pm1 could maintain/shift the overall structure of cisplatin-disrupted gut microbiota toward that of normal control pigs.

Another important issue is to identify the key microorganisms associated with Pm1 intervention leading to the prevention of CKD. After analysis by LEfSe and Spearman's correlations, the genera, *Anaerovibrio*, *possible_genus*_Sk018, and *Holdemanella*, that correlated with improved kidney function also had negative correlations with plasma BUN and creatinine. *Anaerovibrio* has been reported to regulate the absorption of phosphate in the intestine in hemodialysis patients by phosphorus metabolism [50]. Dietary interventions with milk could also affect the abundance of *Anaerovibrio* [51]. Another genus, *Holdemanella*, has been reported to be associated with the progression of CKD and hemodialysis due to the reduction of its abundance in the CKD patients compared with

the health control group [46]. The recent report also observed that *Holdemanella* was attributed to the normal patients instead of hemodialysis patients after LEfSe analysis [52]. Conversely, the genus, *Lachnospiraceae*_UCG_010, had positive correlations with plasma BUN. An increase in *Lachnospiraceae* was observed in immunoglobulin A nephropathy patients, especially in progressive cases [53]. Members of *Lachnospiraceae* families have also been reported to be inversely associated with inflammatory bowel disease in humans by producing butyric acid and to influence the development of obesity and diabetes in germ-free mice [54,55].

In summary, we demonstrated an impressive impact of pretreatment with Pm1 on preventing CKD in a cisplatin-induced kidney injury Lanyu pig model. We further systematically investigated that the preventing effect of Pm1 was associated with reduction of inflammation, apoptosis, and oxidation through regulating the plasma metabolites, IS, creatinine and BUN, via manipulating microbiota. Administration of Pm1 could shift the microbiota to a more even distribution, resulting in a healthy intestinal environment. Pm1-intervention also reduced Gram-negative bacteria, leading to decreased inflammation and apoptosis in the kidney. Additionally, Pm1 demonstrated an influence in the abundances of specific genera, *Anaerovibrio*, *possible_genus*_SK018, *Holdemanella*, and *Lachnospiraceae*_UCG_010 in gut microbiota, which further diversely modulated the specific plasma metabolites, IS, creatinine, and BUN. The reduction of these metabolites could contribute to the prevention/alleviation of the symptoms of CKD. This study highlights the importance of specific probiotic intervention preventing CKD through modulating the tripartite relationship among the host, microbiota, and metabolites. To the best of our knowledge, this is the first trial to use a cisplatin-inducing renal injury pig model to evaluate the effect of Pm1 on preventing renal dysfunction and RPTC apoptosis.

Declaration of Competing Interest

The authors declare no conflict of interest.

Acknowledgments

This work was supported by grants from the Council of Agriculture, Taiwan, Republic of China (108AS-21.1.7-AD-U1). We thank BIOTOOLS Co., Ltd. in Taiwan for kindly assisting with NGS-related analysis.

REFERENCES

[1] Ridaura VK, Faith JJ, Rey FE, Cheng J, Duncan AE, Kau AL, et al. Gut microbiota from twins discordant for obesity modulate metabolism in mice. Science 2013;341:1241214.
[2] Trompette A, Gollwitzer ES, Yadava K, Sichelstiel AK, Sprenger N, Ngom-Bru C, et al. Gut microbiota metabolism of dietary fiber influences allergic airway disease and hematopoiesis. Nat Med 2014;20:159–66.
[3] Campana R, Hemert S, Baffone W. Strain-specific probiotic properties of lactic acid bacteria and their interference with human intestinal pathogens invasion. Gut Pathog 2017;9:12.
[4] Mazmanian SK, Round JL, Kasper DL. A microbial symbiosis factor prevents intestinal inflammatory disease. Nature 2008;453:620–5.
[5] Chen YT, Yang NS, Lin YC, Ho ST, Li KY, Lin JS, et al. A combination of *Lactobacillus mali* APS1 and dieting improved the efficacy of obesity treatment via manipulating gut microbiome in mice. Sci Rep 2018;8:6153.
[6] Chen YP, Lee TY, Hong WS, Hsieh HH, Chen MJ. Effects of *Lactobacillus kefiranofaciens* M1 isolated from kefir grains on enterohemorrhagic *Escherichia coli* infection using mouse and intestinal cell models. J Dairy Sci 2013;96:7467–77.
[7] Hendler R, Zhang Y. Probiotics in the treatment of colorectal cancer. Medicine 2018;5:101.
[8] Jha V, Garcia-Garcia G, Iseki K, Li Z, Naicker S, Plattner B, et al. Chronic kidney disease: global dimension and perspectives. Lancet 2013;382:260–72.
[9] Kotanko P, Carter M, Levin NW. Intestinal bacterial microflora—a potential source of chronic inflammation in patients with chronic kidney disease. Nephrol Dial Transplant 2006;21:2057–60.
[10] Meijers BKI, Evenepoel P. The gut–kidney axis: indoxyl sulfate, *p*-cresyl sulfate and CKD progression. Nephrol Dial Transplant 2011;26:759–61.
[11] Rossi M, Johnson DW, Morrison M, Pascoe EM, Coombes JS, Forbes JM, et al. Synbiotics easing renal failure by improving gut microbiology (SYNERGY): a randomized trial. Clin J Am Soc Nephrol 2016;11:223–31.
[12] Yang J, Lim SY, Ko YS, Lee HY, Oh SW, Kim MG, et al. Intestinal barrier disruption and dysregulated mucosal immunity contribute to kidney fibrosis in chronic kidney disease. Nephrol Dial Transplant 2019;34:419–28.
[13] Fang CY, Lu JR, Chen BJ, Wu C, Chen YP, Chen MJ. Selection of uremic toxin-reducing probiotics *in vitro* and *in vivo*. J Funct Foods 2014;7:407–15.
[14] Nakabayashi I, Nakamura M, Kawakami K, Ohta T, Kato I, Uchida K, et al. Effects of synbiotic treatment on serum level of *p*-cresol in haemodialysis patients: a preliminary study. Nephrol Dial Transplant 2011;26:1094–8.
[15] Larsen N, Vogensen FK, van den Berg FWJ, Nielsen DS, Andreasen AS, Pedersen BK, et al. Gut microbiota in human adults with type 2 diabetes differs from non-diabetic adults. PLoS One 2010;5:e9085.
[16] Giraud S, Favreau F, Chatauret N, Thuillier R, Maiga S, Hauet T. Contribution of large pig for renal ischemia-reperfusion and transplantation studies: the preclinical model. J Biomed Biotechnol 2011;2011:532127.
[17] Yang HC, Zuo Y, Fogo AB. Models of chronic kidney disease. Drug Discov Today Dis Model 2010;7:13–9.
[18] Litten-Brown JC, Corson AM, Clarke L. Porcine models for the metabolic syndrome, digestive and bone disorders: a general overview. Animal 2010;4:899–920.
[19] Cui J, Bai XY, Sun X, Cai G, Hong Q, Ding R, et al. Rapamycin protects against gentamicin-induced acute kidney injury via autophagy in mini-pig models. Sci Rep 2015;5:11256.
[20] Leser TD, Amenuvor JZ, Jensen TK, Lindecrona RH, Boye M, Møller K. Culture-independent analysis of gut bacteria: the pig gastrointestinal tract microbiota revisited. Appl Environ Microbiol 2002;68:673–90.
[21] Misra S, Gordon JD, Fu AA, Glockner JF, Chade AR, Mandrekar J, et al. The porcine remnant kidney model of chronic renal insufficiency. J Surg Res 2006;35:370–9.
[22] Szczurek P, Mosiichuk N, Woliński J, Yatsenko T, Grujic D, Lozinska L, et al. Oral uricase eliminates blood uric acid in the hyperuricemic pig model. PLoS One 2017;12:e0179195.

[23] Wu IW, Hsu KH, Lee CC, Sun CY, Hsu HJ, Tsai CJ, et al. p-Cresyl sulphate and indoxyl sulphate predict progression of chronic kidney disease. Nephrol Dial Transplant 2011;26:938–47.
[24] Wu CY, Jiang YN, Chu HP, Li SH, Wang Y, Li YH, et al. The type I Lanyu pig has a maternal genetic lineage distinct from Asian and European pigs. Anim Genet 2007;38:499–505.
[25] Kuo TY, Lin MJ, Chen LR, Huang LLH. Lanyu minipig is a better model system for studying wound healing. J Biomater Tissue Eng 2015;5:886–94.
[26] Mishra A, Chatterjee US, Mandal TK. Induction of chronic renal failure in goats using cisplatin: a new animal model. Toxicol Int 2013;20:56–60.
[27] Swindle MM, Makin A, Herron AJ, Clubb Jr FJ, Frazier KS. Swine as models in biomedical research and toxicology testing. Vet Pathol 2012;49:344–56.
[28] Wei SH, Chen YP, Chen MJ. Selecting probiotics with the abilities of enhancing GLP-1 to mitigate the progression of type 1 diabetes *in vitro* and *in vivo*. J Funct Foods 2015;18:473–86.
[29] Cianciolo RE, Mohr FC. Urinary system. In: Maxie MG, editor. Jubb, Kennedy and Palmer's pathology of domestic animals. 6th ed., vol. 2. St. Louis: Elsevier; 2016. p. 376–464.
[30] Edgar RC. UPARSE: highly accurate OTU sequences from microbial amplicon reads. Nat Methods 2013;10:996–8.
[31] Wang Q, Garrity GM, Tiedje JM, Cole JR. Naïve bayesian classifier for rapid assignment of rRNA sequences into the new bacterial taxonomy. Appl Environ Microbiol 2007;73:5261–7.
[32] Quast C, Pruesse E, Yilmaz P, Gerken J, Schweer T, Yarza P, et al. The SILVA ribosomal RNA gene database project: improved data processing and web-based tools. Nucleic Acids Res 2013;41:D590–6.
[33] Segata N, Izard J, Waldron L, Gevers D, Miropolsky L, Garrett WS, et al. Metagenomic biomarker discovery and explanation. Genome Biol 2011;12:R60.
[34] Cummings BS, Schnellmann RG. Cisplatin-induced renal cell apoptosis: caspase 3-dependent and -independent pathways. J Pharmacol Exp Ther 2002;302:8–17.
[35] Pabla N, Dong Z. Cisplatin nephrotoxicity: mechanisms and renoprotective strategies. Kidney Int 2008;73:994–1007.
[36] Katagiri D, Hamasaki Y, Doi K, Negishi K, Sugaya T, Nangaku M, et al. Interstitial renal fibrosis due to multiple cisplatin treatments is ameliorated by semicarbazide-sensitive amine oxidase inhibition. Kidney Int 2016;89:374–85.
[37] Yang B, Nahas AME, Thomas GL, Haylor JL, Watson PF, Wagner B, et al. Caspase-3 and apoptosis in experimental chronic renal scarring. Kidney Int 2001;60:1765–76.
[38] Khalilzadeh B, Shadjou N, Kanberoglu GS, Afsharan H, de la Guardia M, Charoudeh HN, et al. Advances in nanomaterial based optical biosensing and bioimaging of apoptosis via caspase-3 activity: a review. Mikrochim Acta 2018;185:434.
[39] Kumar NSN, Balamurugan R, Jayakanthan K, Pulimood A, Pugazhendhi S, Ramakrishna BS. Probiotic administration alters the gut flora and attenuates colitis in mice administered dextran sodium sulfate. J Gastroenterol Hepatol 2008;23:1834–9.
[40] Vaziri ND, Wong J, Pahl M, Piceno YM, Yuan J, DeSantis TZ, et al. Chronic kidney disease alters intestinal microbial flora. Kidney Int 2013;83:308–15.
[41] Koppe L, Mafra D, Fouque D. Probiotics and chronic kidney disease. Kidney Int 2015;88:958–66.
[42] Ramezani A, Raj DS. The gut microbiome, kidney disease, and targeted interventions. J Am Soc Nephrol 2014;25:657–70.
[43] Cigarrán S, Neches C, Lamas JM, García-Trio G, Alonso M, Saavedra J. A case report of a pyogenic liver abscess caused by *Fusobacterium nucleatum* in a patient with autosomal dominant polycystic kidney disease undergoing hemodialysis. Ther Apher Dial 2008;12:91–5.
[44] Antonic V, Stojadinovic A, Kester KE, Weina PJ, Brücher BL, Protic M, et al. Significance of infectious agents in colorectal cancer development. J Cancer 2013;4:227–40.
[45] Hida M, Aiba Y, Sawamura S, Suzuki N, Satoh T, Koga Y. Inhibition of the accumulation of uremic toxins in the blood and their precursors in the feces after oral administration of Lebenin, a lactic acid bacteria preparation, to uremic patients undergoing hemodialysis. Nephron 1996;74:349–55.
[46] Lun H, Yang W, Zhao S, Jiang M, Xu M, Liu F, et al. Altered gut microbiota and microbial biomarkers associated with chronic kidney disease. Microbiology 2019;8:e678.
[47] Kieffer DA, Piccolo BD, Vaziri ND, Liu S, Lau WL, Khazaeli M, et al. Resistant starch alters gut microbiome and metabolomic profiles concurrent with amelioration of chronic kidney disease in rats. Am J Physiol Renal Physiol 2016;310:F857–71.
[48] den Besten G, van Eunen K, Groen AK, Venema K, Reijngoud D, Bakke BM. The role of short-chain fatty acids in the interplay between diet, gut microbiota, and host energy metabolism. J Lipid Res 2013;54:2325–40.
[49] Peng L, Li Z, Green RS, Holzman IR, Lin J. Butyrate enhances the intestinal barrier by facilitating tight junction assembly via activation of AMP-activated protein kinase in Caco-2 cell monolayers. J Nutr 2009;139:1619–25.
[50] Miao YY, Xu CM, Xia M, Zhu HQ, Chen YQ. Relationship between gut microbiota and phosphorus metabolism in hemodialysis patients: a preliminary exploration. Chin Med J 2018;131:2792–9.
[51] Rojo D, Méndez-García C, Raczkowska BA, Bargiela R, Moya A, Ferrer M, et al. Exploring the human microbiome from multiple perspectives: factors altering its composition and function. FEMS Microbiol Rev 2017;41:453–78.
[52] Stadlbauer V, Horvath A, Ribitsch W, Schmerböck B, Schilcher G, Lemesch S, et al. Structural and functional differences in gut microbiome composition in patients undergoing haemodialysis or peritoneal dialysis. Sci Rep 2017;7:15601.
[53] De Angelis M, Montemurno E, Piccolo M, Vannini L, Lauriero G, Maranzano V, et al. Microbiota and metabolome associated with immunoglobulin A nephropathy (IgAN). PLoS One 2014;9:e99006.
[54] Barrios C, Beaumont M, Pallister T, Villar J, Goodrich JK, Clark A, et al. Gut-microbiota-metabolite axis in early renal function decline. PLoS One 2015;10:e0134311.
[55] Kameyama K, Itoh K. Intestinal colonization by a Lachnospiraceae Bacterium contributes to the development of diabetes in obese mice. Microb Environ 2014;29:427–30.